Transcriptional profiling and functional characterization of three genetic variants in *SLC16A2* gene

L. Esposito[1,2], F. Rey[1,2], E. Maghraby[1,3], L. Messa[2,4], M. Elli[1,2], F. Bruschi[5,6], G. Zuccotti[1,7], L. Alberti[2], D. Tonduti[5,6], S. Carelli[1,2,*], C. Cereda[2,*]

1 Pediatric Clinical Research Center "Romeo ed Enrica Invernizzi", Department of Biomedical and Clinical Sciences, University of Milan, Milan, Italy.
2 Center of Functional Genomics and Rare Diseases, Department of Pediatrics, Buzzi Children's Hospital, Milan, Italy.
3 Department of Biology and Biotechnology "L. Spallanzani", University of Pavia, Pavia, Italy.
4 Department of Electronics, Information and Bioengineering (DEIB), Politecnico di Milano, Milan, Italy.
5 Unit of Pediatric Neurology, C.O.A.L.A. (Center for Diagnosis and Treatment of Leukodystrophies), V. Buzzi Children's Hospital, Milan, Italy
6 Department of Biomedical and Clinical Sciences, University of Milan, Milan, Italy
7 Department of Pediatrics, Children's Hospital "V. Buzzi", Milan, Italy.
* These authors contributed equally to the work.

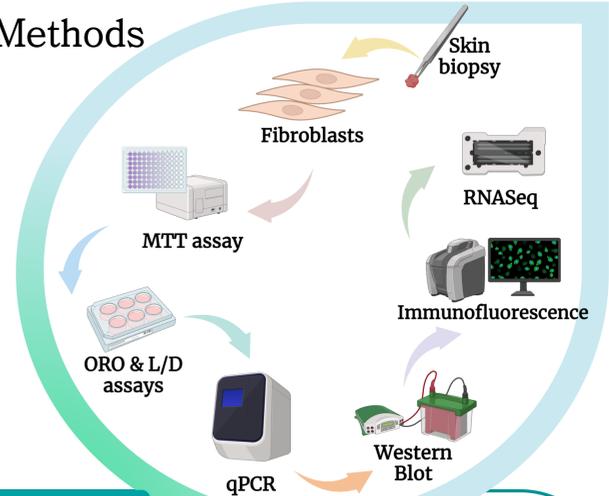**SIGU Società Italiana di Genetica Umana**

Introduction

Genetics variants in *SLC16A2* gene encoding for the monocarboxylate transporter 8 (MCT8) cause a severe X-linked intellectual deficit known as Allan–Herndon–Dudley syndrome (AHDS). MCT8 promotes cellular uptake and efflux of thyroid hormones. Active T3 and retinoid X receptors (RXRs) can form heterodimer complexes which bind to hormone response elements (HREs) leading to activation or repression of transcription.

Aim of the study

The main aim is to investigate the impact of MCT8 mutations on the pathogenetic mechanisms of AHDS.

ID	Gender	Date of birth	Mutation	Type of Mutation
AHDS_1	M	04/07/2018	NM_006517: c.430+ 1G>A	Splicing Variant
AHDS_2	M	02/04/2010	NM_006517:c.169 0G>A (p.Gly564Arg)	Missense
AHDS_3	M	28/03/2018	NM:006517-5: c.623G>A; (p.Gly208Asp)	Missense

Methods

Results
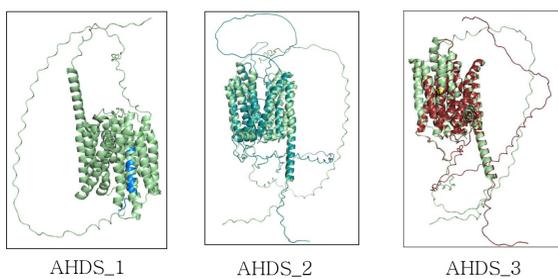
Protein prediction

Figure 1. Prediction and modelling of the three different mutated MCT8 performed by AlphaFold2 and visualized with PyMOL software.
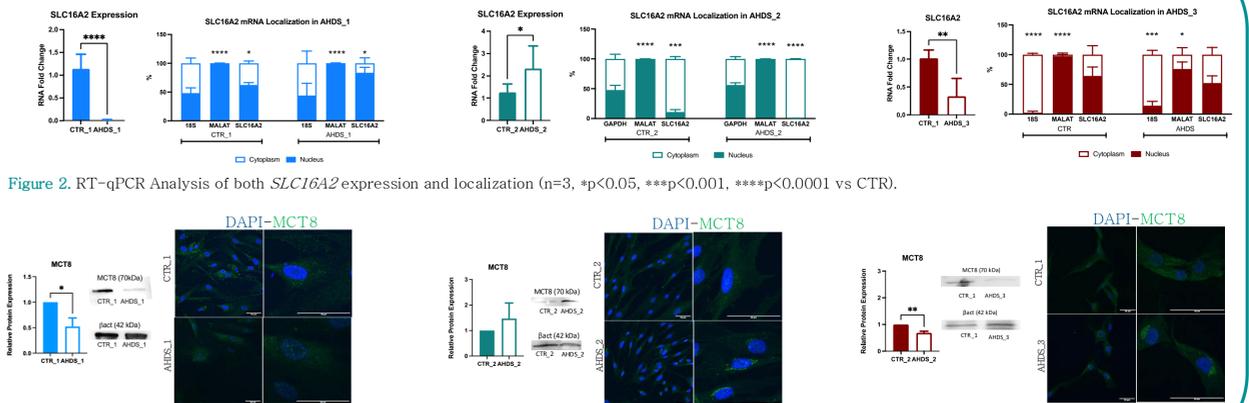
MCT8 characterization

Figure 2. RT-qPCR Analysis of both *SLC16A2* expression and localization (n=3, *p<0.05, ***p<0.001, ****p<0.0001 vs CTR).

Figure 3. MCT8 expression via western blot and immunofluorescence (n=3, *p<0.05 vs CTR, **p<0.01).
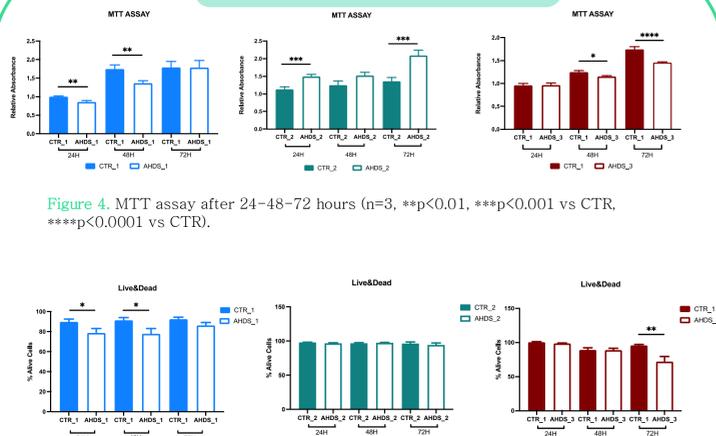
Cell metabolism

Figure 4. MTT assay after 24-48-72 hours (n=3, **p<0.01, ***p<0.001 vs CTR, ****p<0.0001 vs CTR).

Figure 5. Live&Dead assay revealed a decrease in live cell populations (n=3, *p<0.05 vs CTR, **p<0.01).

RNA-Seq

Figure 8. Heatmap of DEGs.

Figure 9. Number of DEGs that emerged after RNA-seq, divided for biotype and FC entity.

Figure 10. DEGs Gene Biotype.

Figure 11. Biological Processes Gene Ontology for DEGs.

Figure 12. Cellular Component Gene Ontology for DEGs.

Signaling

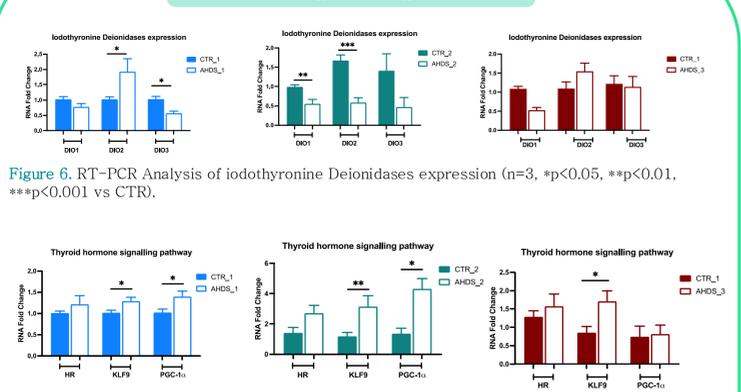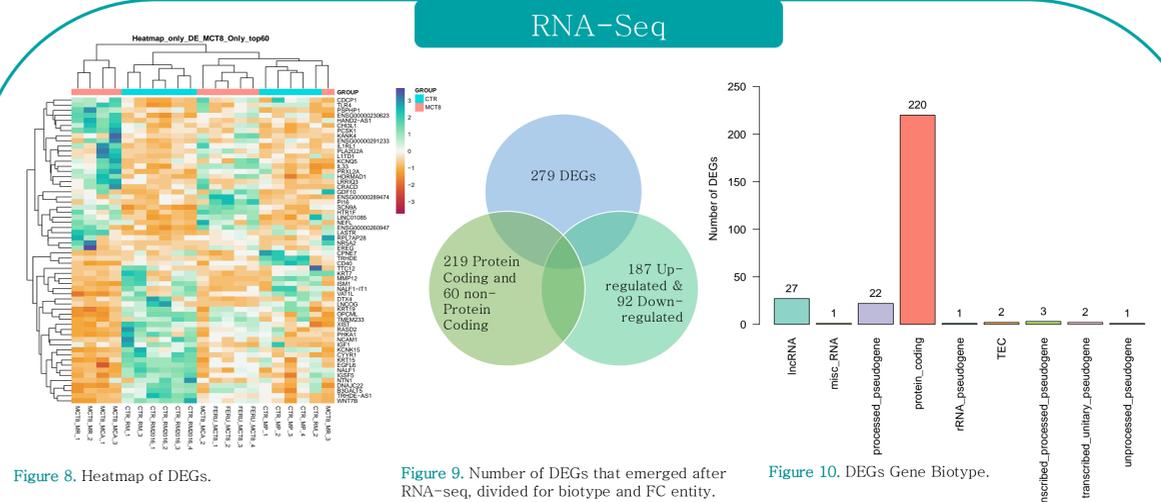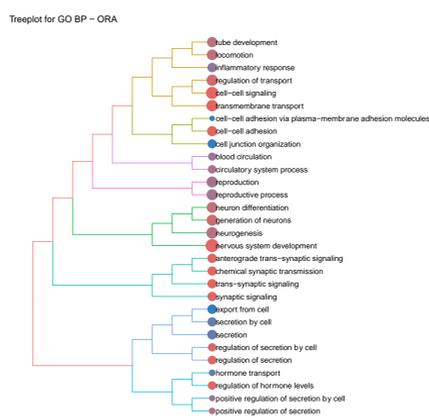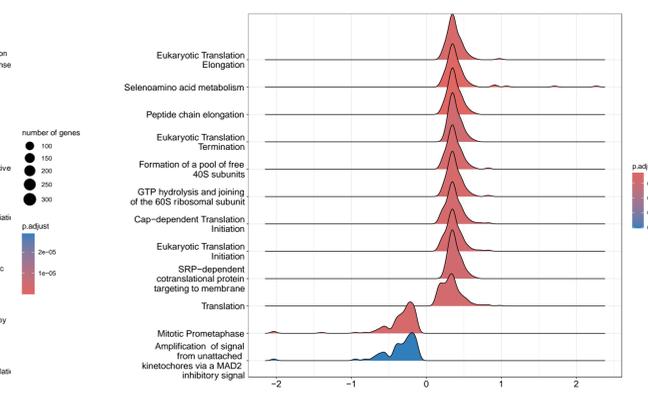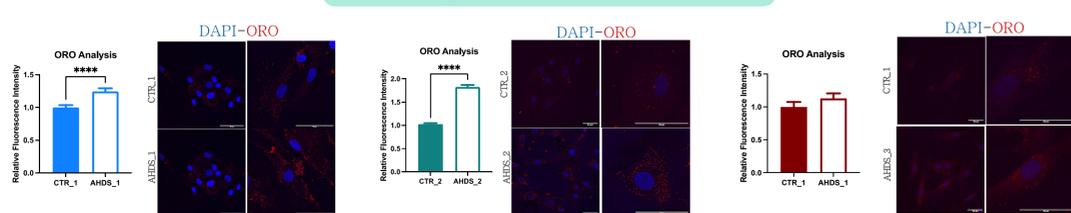

Figure 6. RT-PCR Analysis of iodothyronine Deionidases expression (n=3, *p<0.05, **p<0.01, ***p<0.001 vs CTR).

Figure 7. RT-PCR Analysis of thyroid hormone signaling pathway expression (n=3, *p<0.05, **p<0.01, ***p<0.001 vs CTR).

Lipid accumulation

Figure 13. The Oil Red O staining revealed an increasing presence of lipid droplets (****p<0.0001 vs CTR).
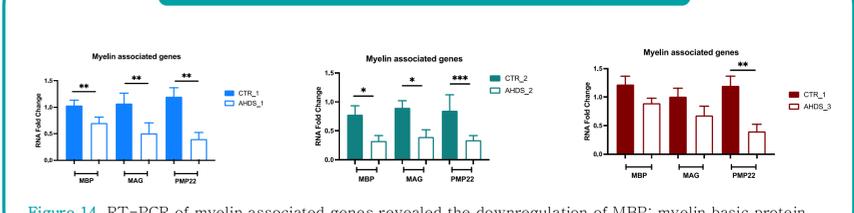
Impact on myelin associated genes

Figure 14. RT-PCR of myelin associated genes revealed the downregulation of MBP: myelin basic protein, myelin associated glycoprotein and PMP22: Peripheral myelin protein 22 (n=3, *p<0.05, **p<0.01 vs CTR).

Conclusions

Our data emphasize a mutation-specific impairment in patients' primary fibroblasts which can be used as pre-clinical experimental model of this rare disease.